Modeling The Thickness And Shape Of Lunar Volatile Stability Zones

Hunter Danque and Kevin Cannon

Thursday June 9, 2022

Outline

- Introduction
- Background
- Methods
- Results
  - Physical and Thermal models
  - Topographic diffusion and real crater profiles
- Conclusions

Hypotheses

- Volatiles may experience subsurface temperatures that could sublimate ice from the base of cold traps
- Temperature conditions may exist to redeposit and concentrate volatiles in predictable parts of subsurface cold traps
- There may be a positive feedback mechanism in which increased ice content at the base of volatile stability improves the thermal conductivity and thickens volatile stability zones

Background – Cold Traps

- The water ice stability zone exists where:
  - regolith surface temperatures are below ~110 K
  - subsurface temperatures are below **~145 K**
  - these conditions occur in some polar regions on the Moon
- They are often found in Permanently Shadowed Regions (PSRs) that may host cold traps
- The threshold for defining a cold trap is a sublimation rate of 1 kg m^{-2} Ga^{-1}

(Schorghofer and Aharonson, 2014; Siegler et al., 2011; Zhang and Paige, 2009)

Illumination and Temperature of a PSR

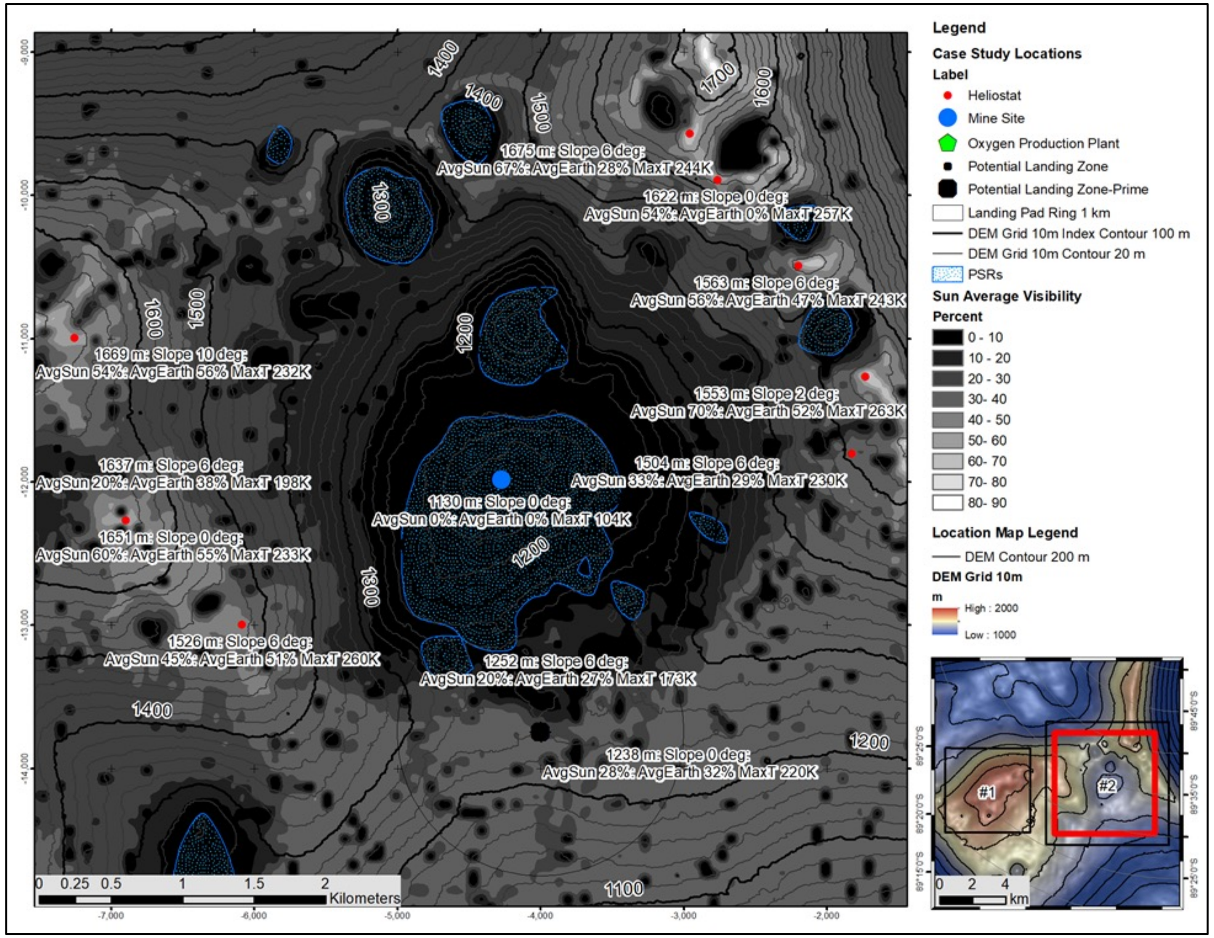

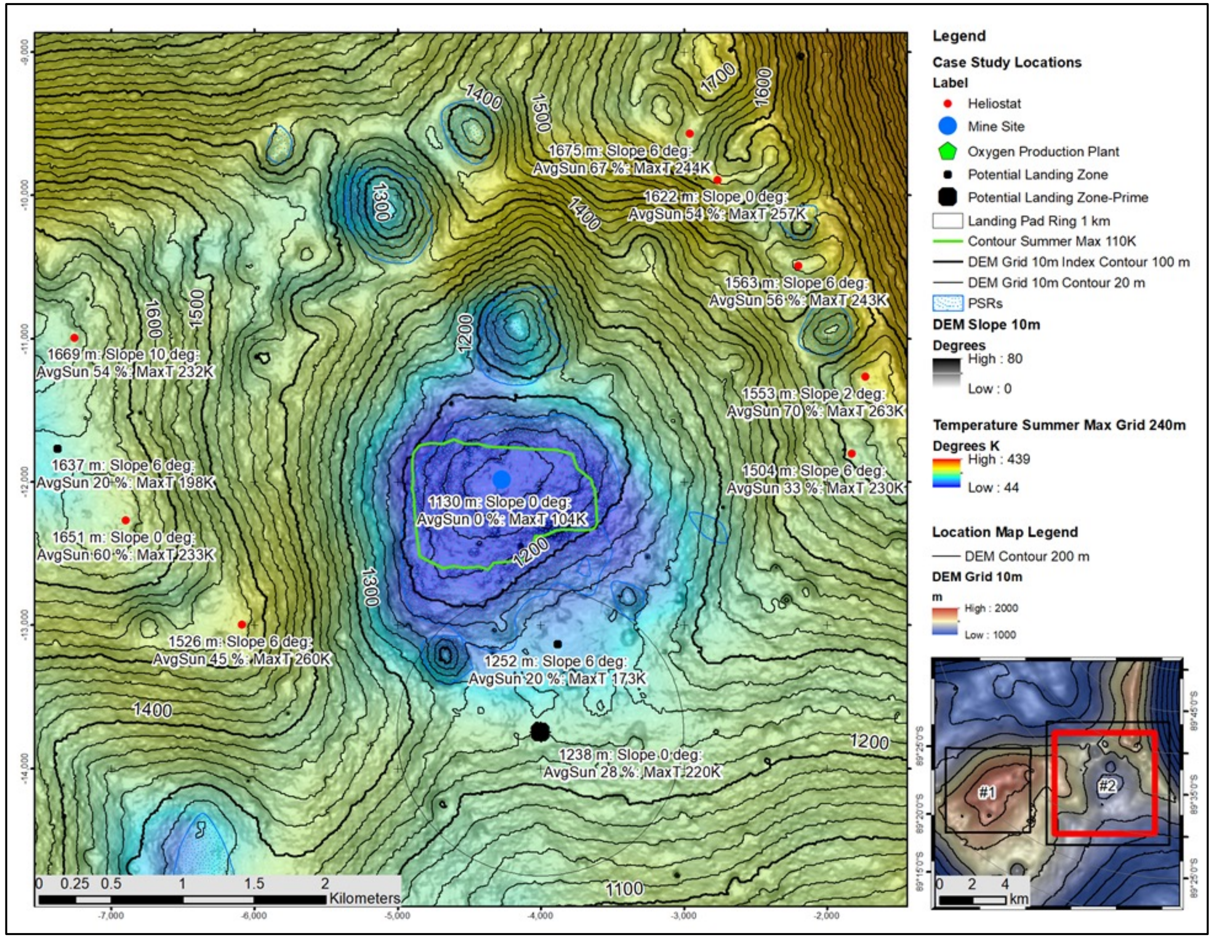

Background – Obliquity and TPW

- About 3±1 Ga the Moon was at half its current semimajor axis
- The Moon may have experienced a Cassini State 1 to 2 transition and experienced obliquity as high as 77 degrees and extended periods at 25-50 degrees
- The Moon may have experienced true polar wander (TPW) with evidence for a paleopole at about 3.5 Ga
- During TPW the planet/moon realigns the rotation axis to the maximum principal axis of inertia when there is a change in internal mass distribution

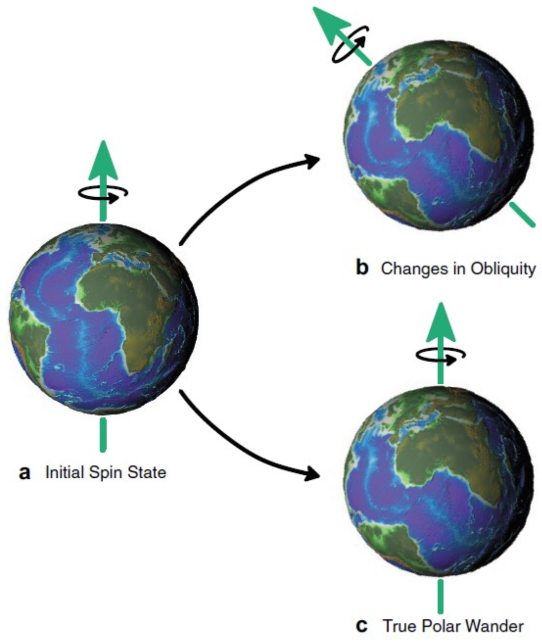

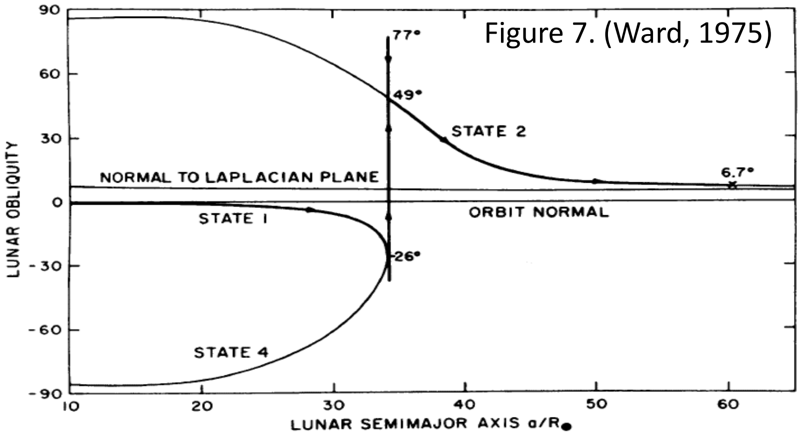

Figure 7. (Ward, 1975)

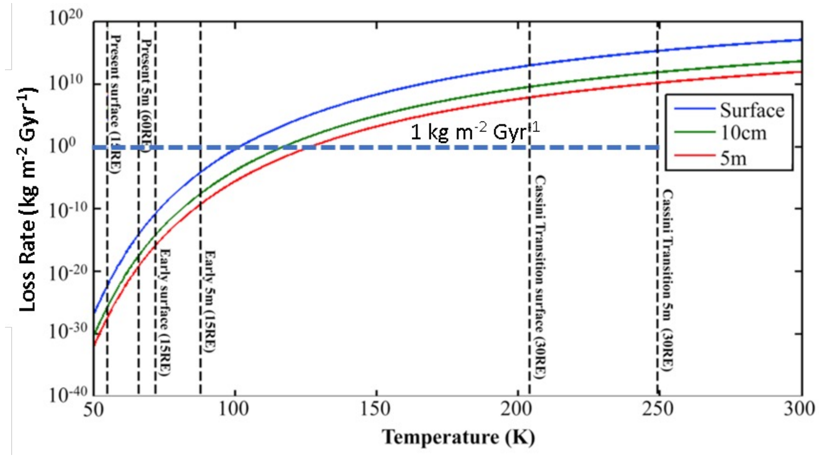

(Siegler et al., 2016; 2011, Ward 1975)

Background – Hydrogen and Ice Depth

- Hydrogen in upper meter from epithermal neutron data (a. b.)
- Calculated current and paleo pole depth to ice stability (c. d.)
- Combined current and paleo pole ice depths match the hydrogen content well (e. f.)

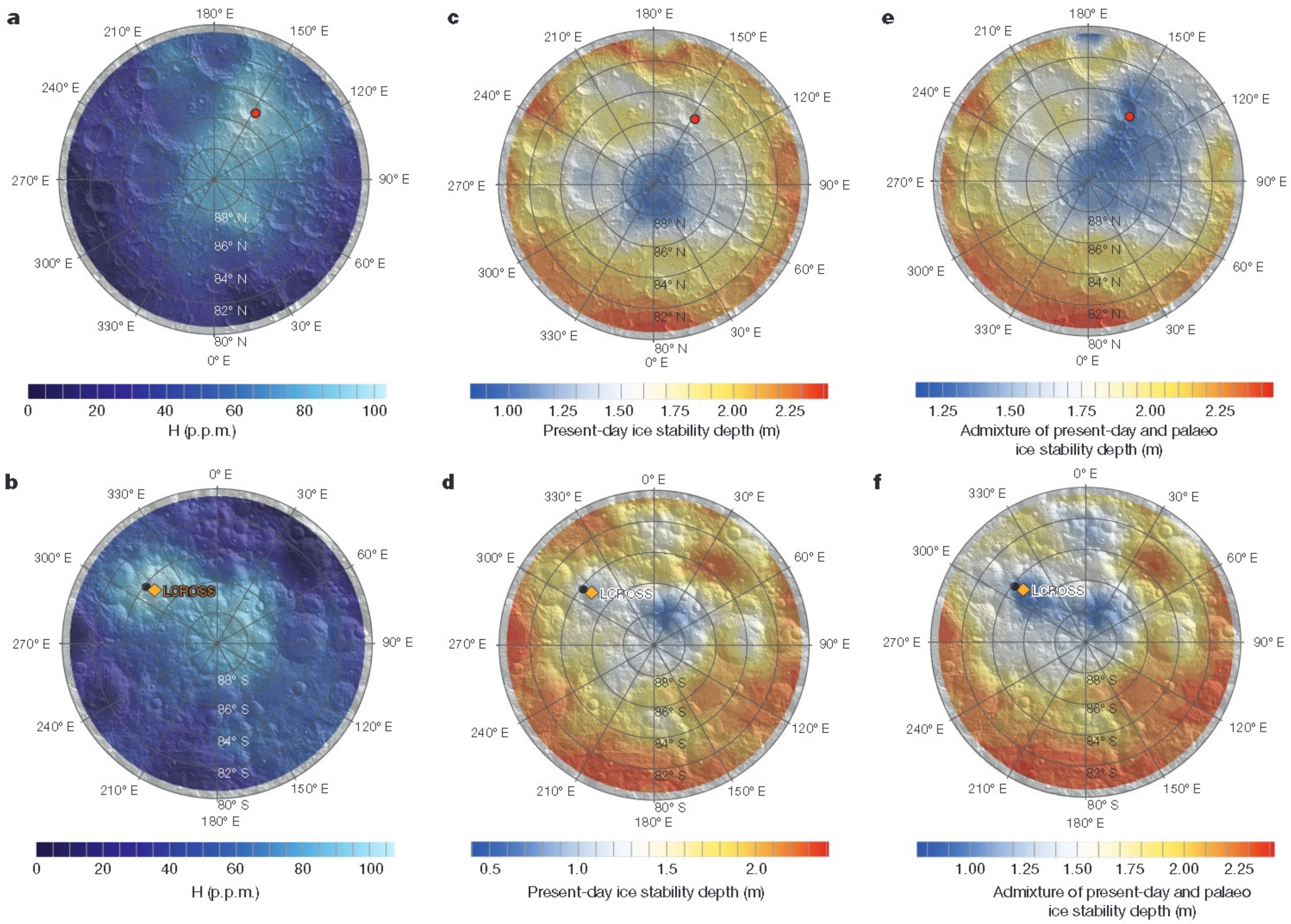

(Siegler et al., 2016)

Background - Topographic Diffusion

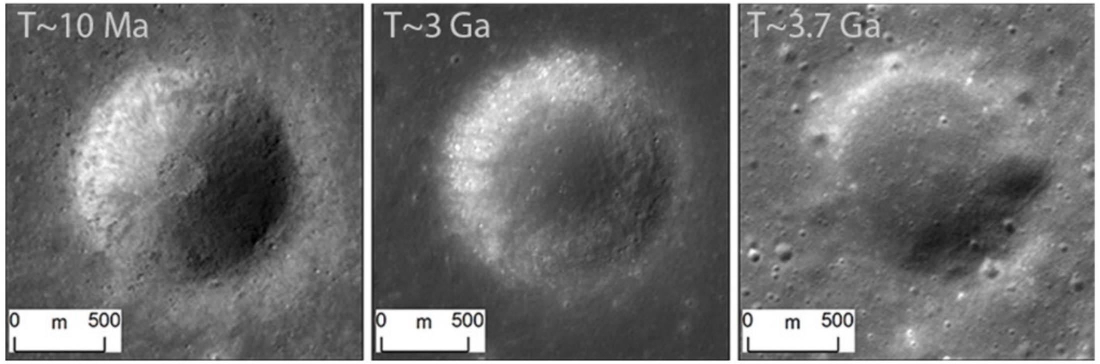

- Example of craters change in infill thickness and slope as a function of time
- $\frac{dh}{dt} = \kappa \nabla^2 h$, where κ is the diffusivity

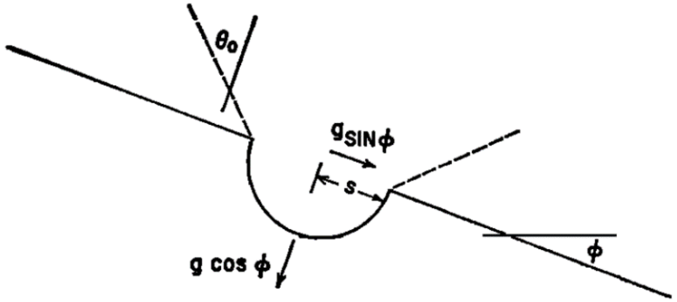

- Conceptual setup of a small impactor on the slope of a larger crater or hillside
- There is a net translation of mass in the downslope direction

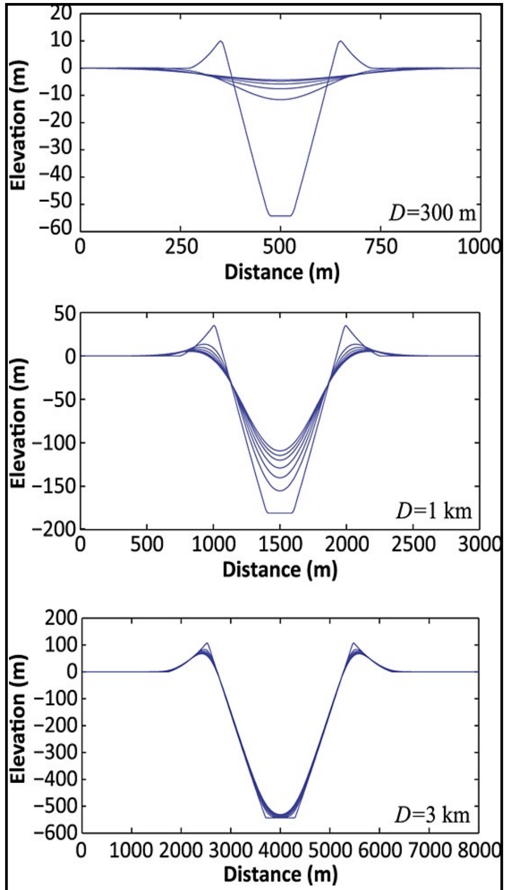

- Crater diameter and fill thickness

(Fassett et al., 2018; Fassett and Thomson, 2014; Soderblom, 1970)

Methods-Model Properties

- Thermal conductivity (k)
  - Ice @ 110 K = 5.5 W m^{-1} K^{-1}
  - Regolith = 0.023 W m^{-1} K^{-1}
  - Upper Megaregolith= 0.2 W m^{-1} K^{-1}
  - Lower Megaregolith= 1.0 to 2.0 W m^{-1} K^{-1}
- Density
  - Ice @ 110 K = 932 kg m^{-3}
  - Regolith = 1100-1800 kg m^{-3}
  - Upper Megaregolith= 1960-2600 kg m^{-3}
  - Lower Megaregolith= 2600-2900 kg m^{-3}

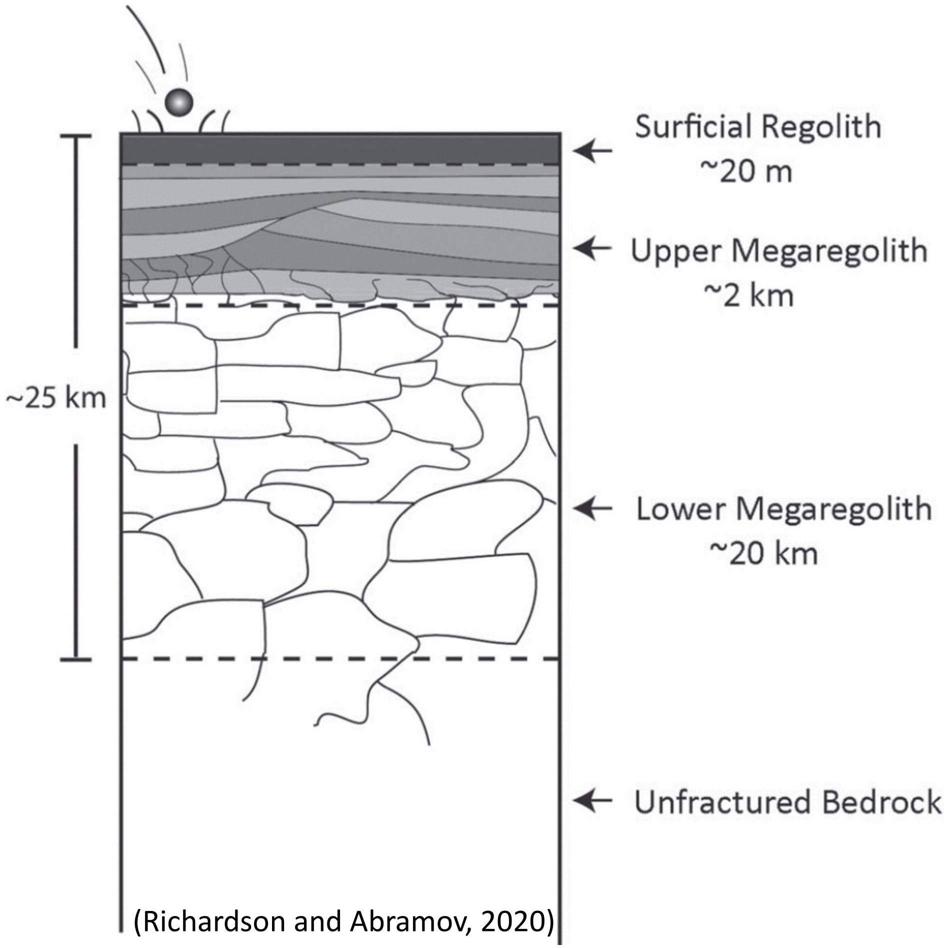

(Richardson and Abramov, 2020)

(Keihm and Langseth, 1975; Warren and Rasmussen, 1987; Carnahan et al., 2021)

Initial Synthetic Crater

Thermal diffusivity
$\alpha = k/\rho c_p$
  k is thermal conductivity
  ρ is density
  c_p is heat capacity

Upper Boundary conditions are:

- 110 K cold trap
- 160 K illuminated

Lower Boundary condition is 90 K/km

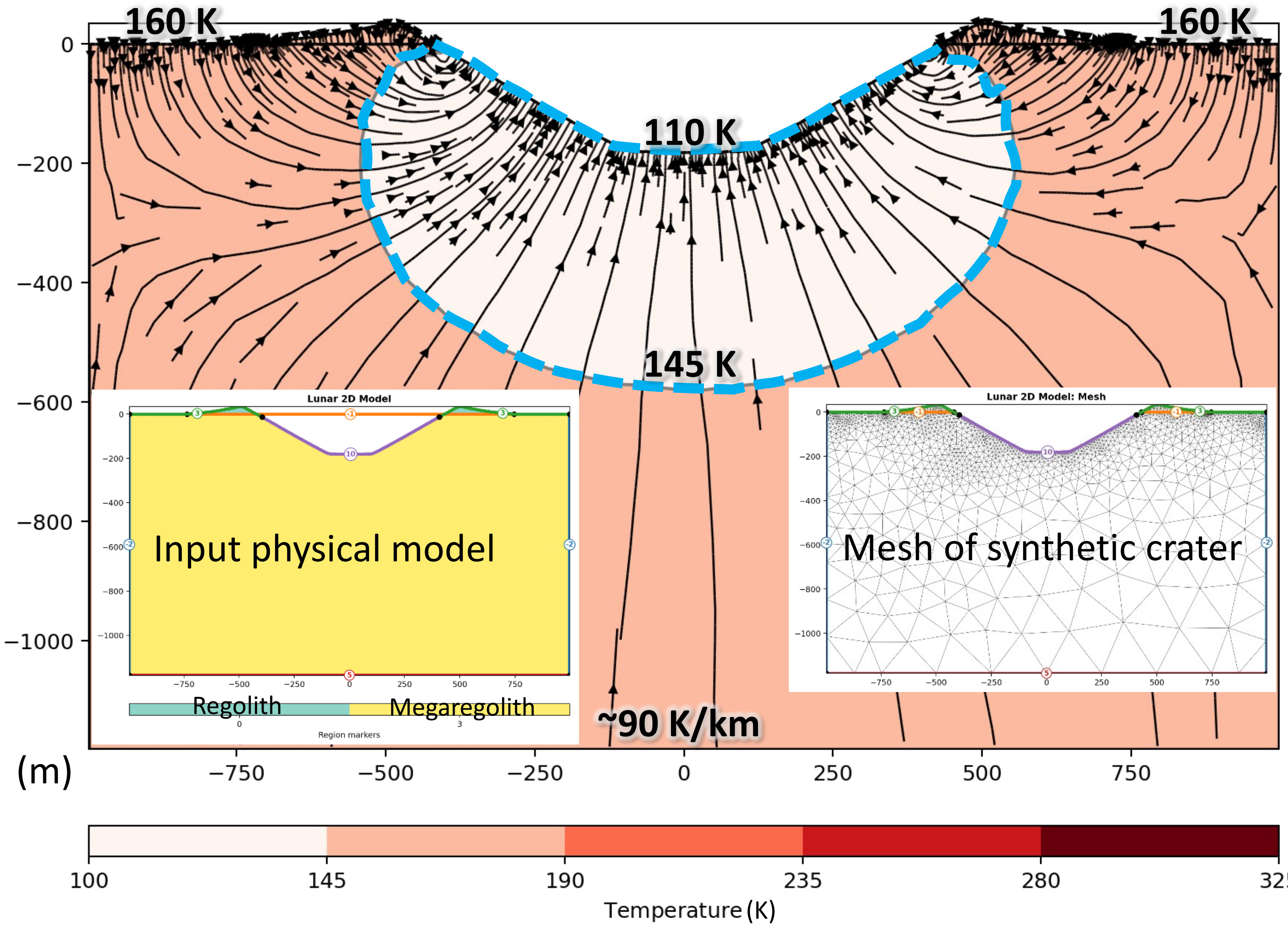

Original water ice stability zone

Int. Crater= -181 m

160 , Temperature (K)
0.023 , Thermal Conductivity (W/m/K)
1800 , Input Density (kg/m^3)
448 , Heat Capacity (J kg-1 K-1)
2.84e-08 , Thermal Diffusivity (m^2/s)

110 , Temperature (K)
0.023 , Thermal Conductivity (W/m/K)
1800 , Input Density (kg/m^3)
307 , Heat Capacity (J kg-1 K-1)
4.15e-08 , Thermal Diffusivity (m^2/s)

(Rücker et al., 2017)

Filled Synthetic Crater

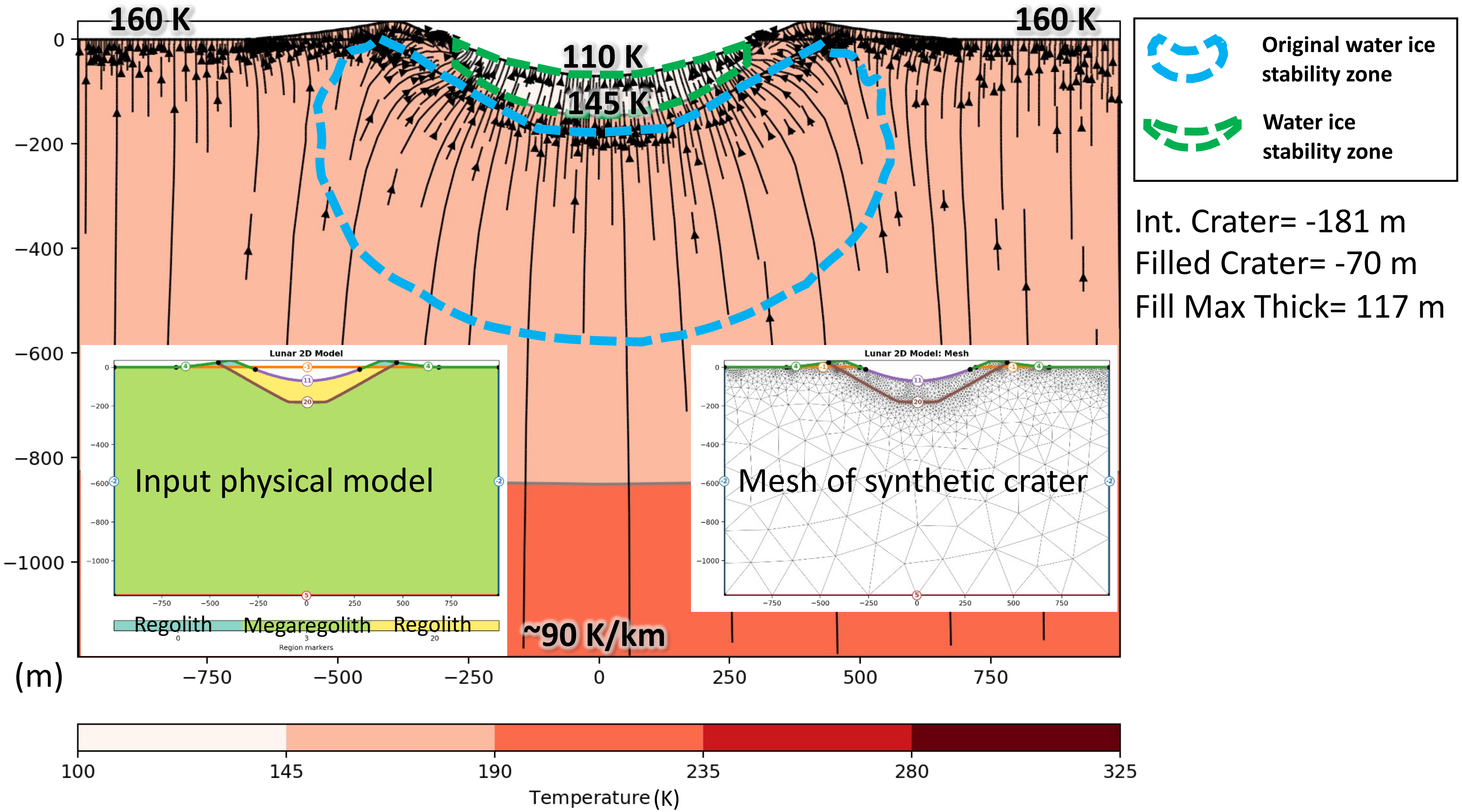

Int. Crater= -181 m
Filled Crater= -70 m
Fill Max Thick= 117 m

(Rücker et al., 2017)

Filled Synthetic Crater

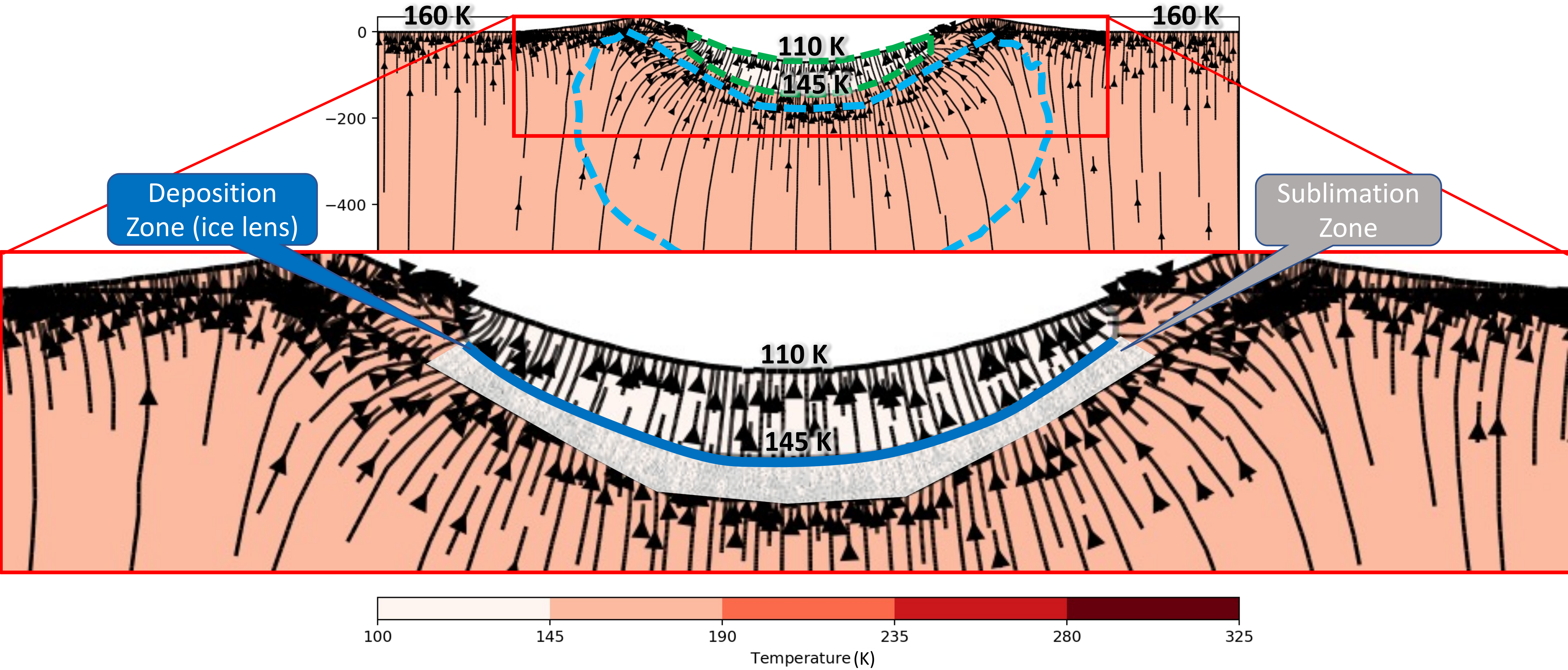

(Rücker et al., 2017)

Filled Synthetic Crater with ice

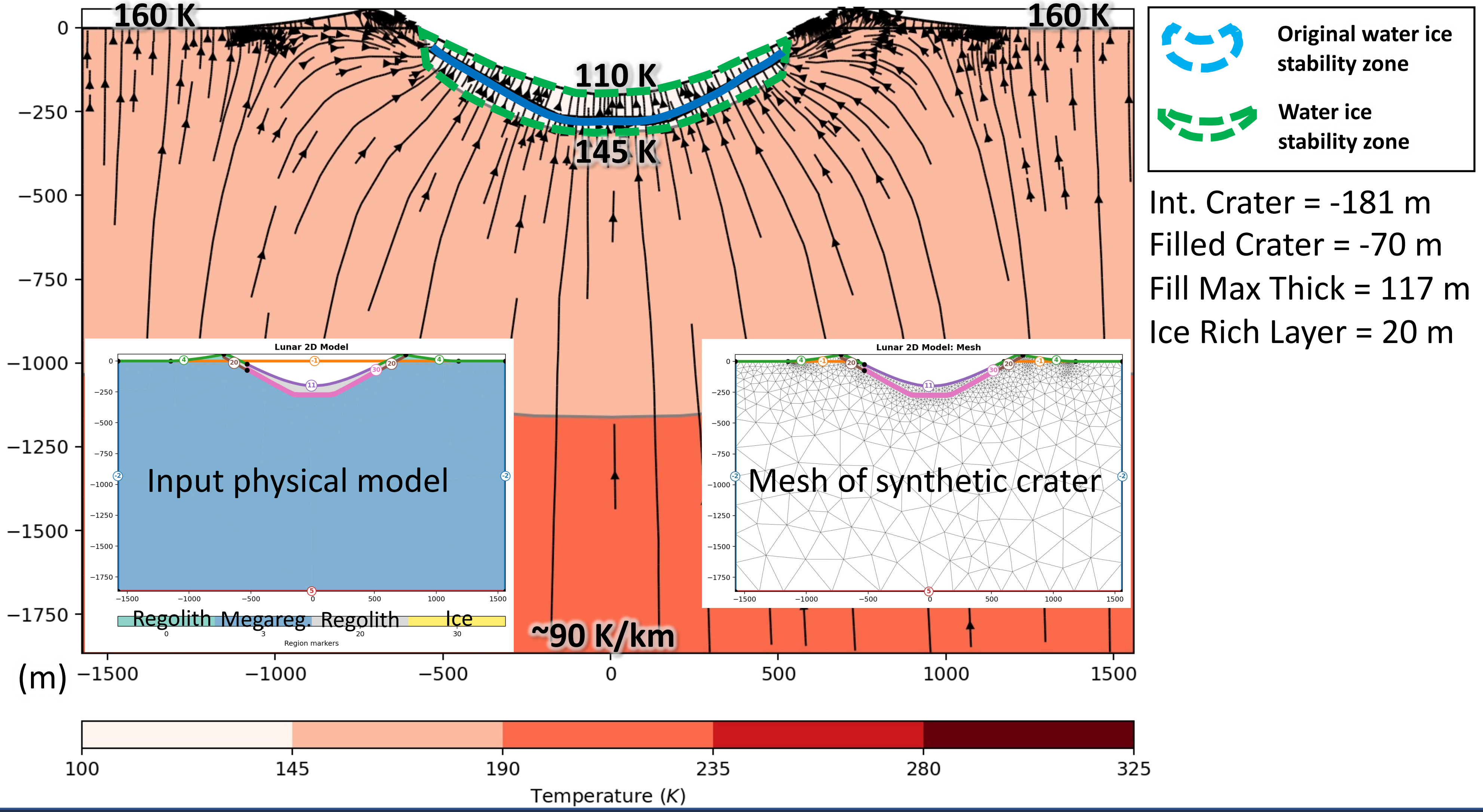

Int. Crater = -181 m
Filled Crater = -70 m
Fill Max Thick = 117 m
Ice Rich Layer = 20 m

(Rücker et al., 2017)

Crater - VIPER Mission Area

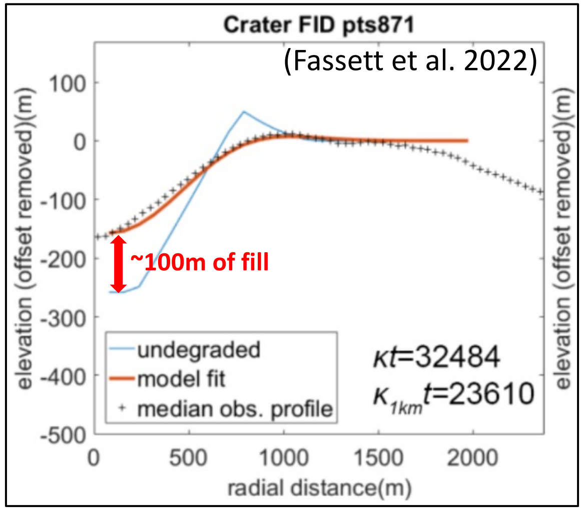

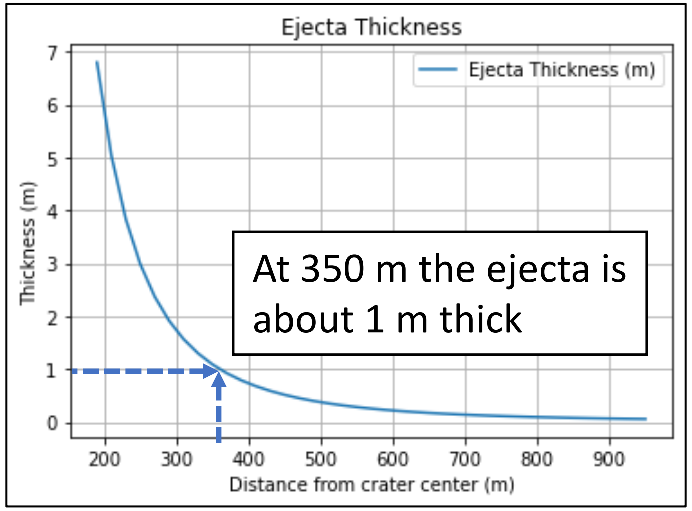

Ejecta thickness $t = 0.14\, R^{0.74}(r/R)^{-3.0}$

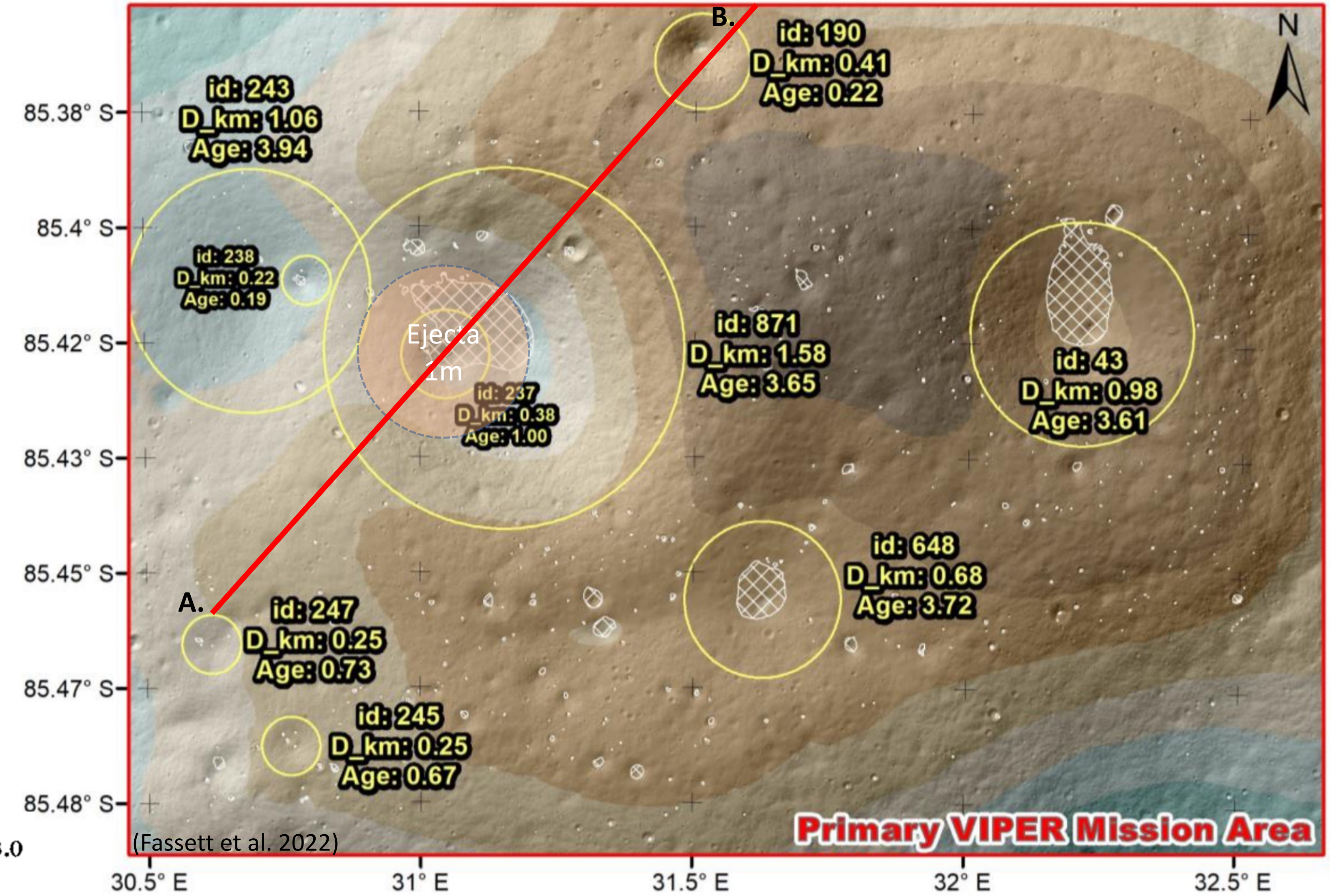

Crater - VIPER Mission Area

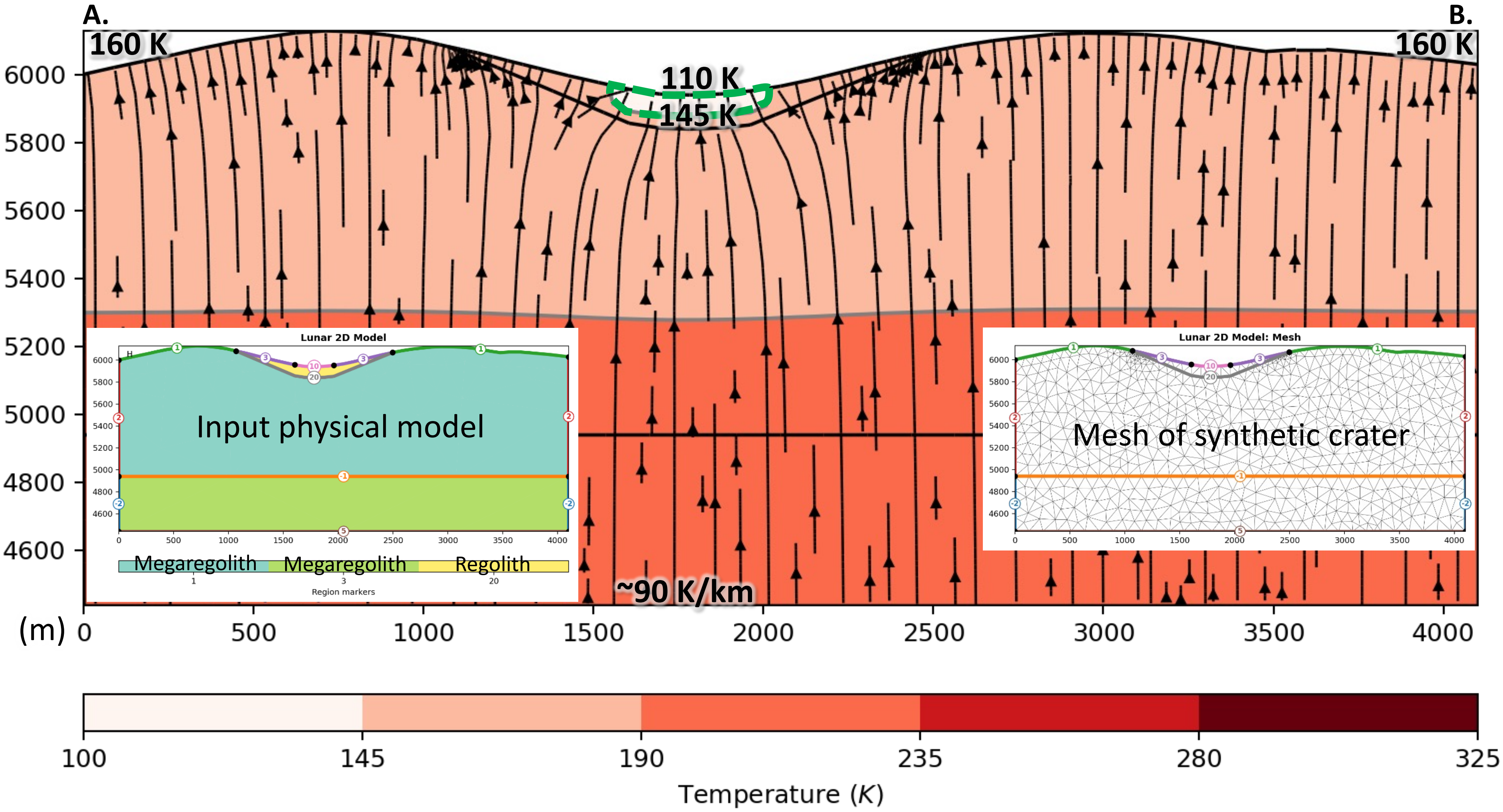

Lunar volatile system timeline – VIPER area example

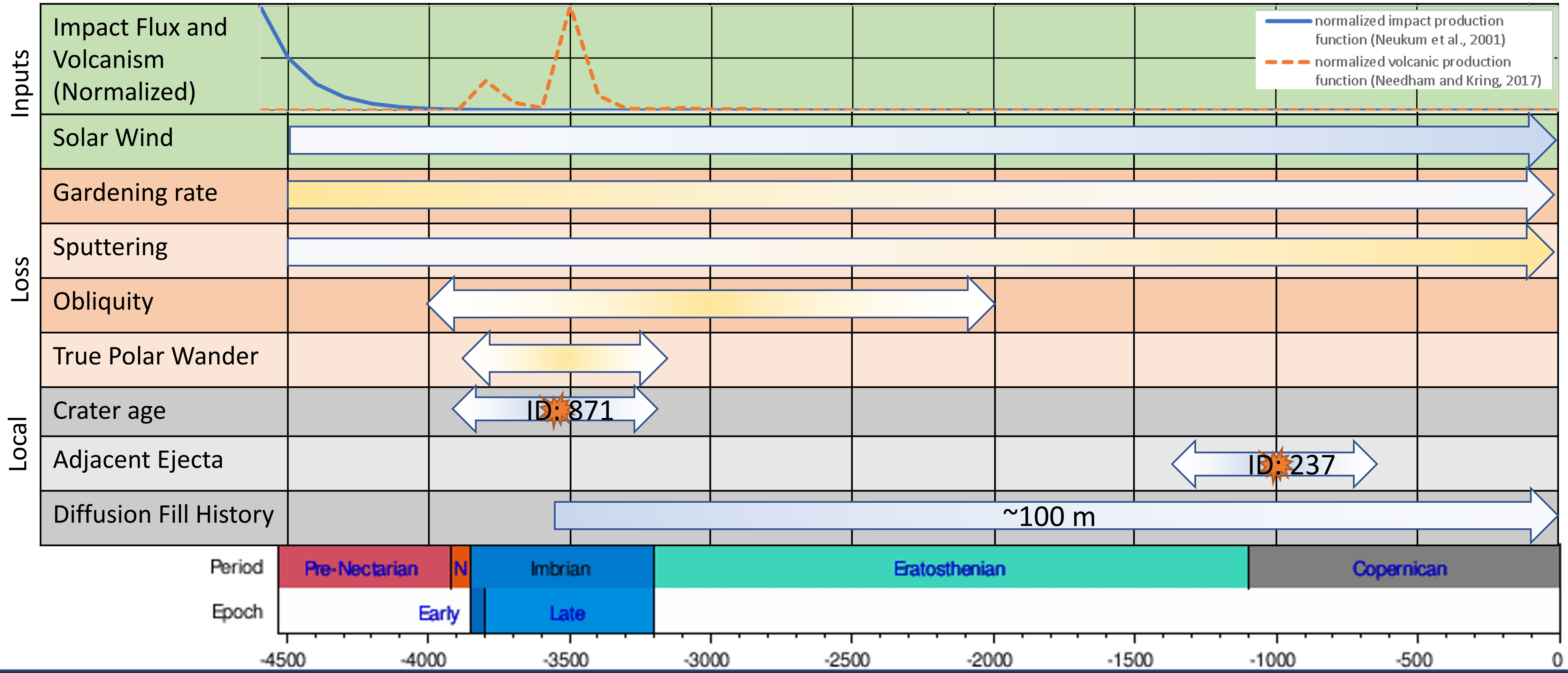

Conclusion

- The results appear to support potential for remobilization and concentration of water ice near the base of volatile stability
- Future work will develop and improve:
  - Physical crater fill thickness estimates from diffusion and ejecta fill
  - Volatile concentration scenarios

References

Carnahan, E., Wolfenbarger, N.S., Jordan, J.S., Hesse, M.A., 2021. New insights into temperature-dependent ice properties and their effect on ice shell convection for icy ocean worlds. Earth and Planetary Science Letters 563, 116886. https://doi.org/10.1016/j.epsl.2021.116886

Fassett, C.I., Beyer, Heldmann, L., Hirabayashi, T., Keszthelyi, L., Lim, D.S.S., 2022. Age Estimates for Permanently Shadowed Craters in the Viper Mission Area. Presented at the 53rd LPSC, p. 2.

Fassett, C.I., Crowley, M.C., Leight, C., Dyar, M.D., Minton, D.A., Hirabayashi, M., Thomson, B.J., Watters, W.A., 2017. Evidence for rapid topographic evolution and crater degradation on Mercury from simple crater morphometry. Geophysical Research Letters 44, 5326–5335. https://doi.org/10.1002/2017GL073769

Fassett, C.I., Thomson, B.J., 2014. Crater degradation on the lunar maria: Topographic diffusion and the rate of erosion on the Moon. Journal of Geophysical Research: Planets 119, 2255–2271. https://doi.org/10.1002/2014JE004698

Heiken, G.H., Vaniman, D.T., French, B.M., 1991. Lunar sourcebook - A user's guide to the Moon. Cambridge University Press.

Keihm, S.J., Langseth, M.G., 1975. Microwave Emission Spectrum of the Moon: Mean Global Heat Flow and Average Depth of the Regolith. Science 187, 64–66. https://doi.org/10.1126/science.187.4171.64

McGetchin, T.R., Settle, M., Head, J.W., 1973. Radial thickness variation in impact crater ejecta: implications for lunar basin deposits. Earth and Planetary Science Letters 20, 226–236. https://doi.org/10.1016/0012-821X(73)90162-3

Rücker, C., Günther, T., Wagner, F.M., 2017. pyGIMLi: An open-source library for modelling and inversion in geophysics. Computers & Geosciences 109, 106–123. https://doi.org/10.1016/j.cageo.2017.07.011

Schorghofer, N., Aharonson, O., 2014. The Lunar Thermal Ice Pump. ApJ 788, 169. https://doi.org/10.1088/0004-637X/788/2/169

Siegler, M., Nagihara, S., Grott, M., Warren, P.H., Paige, D.A., Kiefer, W.S., Smrekar, S.E., Wieczorek, M.A., 2020. Lunar Heat Flow: Global Predictions and Reduced Heat Flux (Working Paper).

Siegler, M.A., Bills, B.G., Paige, D.A., 2011. Effects of orbital evolution on lunar ice stability. Journal of Geophysical Research: Planets 116. https://doi.org/10.1029/2010JE003652

Siegler, M.A., Miller, R.S., Keane, J.T., Laneuville, M., Paige, D.A., Matsuyama, I., Lawrence, D.J., Crotts, A., Poston, M.J., 2016. Lunar true polar wander inferred from polar hydrogen. Nature 531, 480–484. https://doi.org/10.1038/nature17166

Soderblom, L.A., 1970. A model for small-impact erosion applied to the lunar surface. Journal of Geophysical Research (1896-1977) 75, 2655–2661. https://doi.org/10.1029/JB075i014p02655

Ward, W.R., 1975. Past Orientation of the Lunar Spin Axis. Science 189, 377–379. https://doi.org/10.1126/science.189.4200.377

Warren, P.H., Rasmussen, K.L., 1987. Megaregolith insulation, internal temperatures, and bulk uranium content of the moon. Journal of Geophysical Research: Solid Earth 92, 3453–3465. https://doi.org/10.1029/JB092iB05p03453

Zhang, J.A., Paige, D.A., 2009. Cold-trapped organic compounds at the poles of the Moon and Mercury: Implications for origins. Geophysical Research Letters 36, 5.